

COLLISION ANALYSIS FOR MULTIPLE SATELLITES RELEASED FROM A COMMON DISPENSER

Antonio D'Anniballe⁽¹⁾, Leonard Felicetti⁽²⁾, Stephen Hobbs⁽³⁾

⁽¹⁾*Cranfield University, College Road, Cranfield, MK43 0AL, UK,
antonio.danniballe@cranfield.ac.uk*

⁽²⁾*Cranfield University, College Road, Cranfield, MK43 0AL, UK, leonard.felicetti@cranfield.ac.uk*

⁽³⁾*Cranfield University, College Road, Cranfield, MK43 0AL, UK, s.e.hobbs@cranfield.ac.uk*

ABSTRACT

The number of small spacecraft launched to space has increased dramatically in the past few years, and with the emergence of mega-constellations it is projected to increase even more in the coming decades. Small satellites are usually launched together in rideshare launches and released from a common dispenser when reaching nominal orbit. Due to the lack of available measurement and control capabilities, the release phase is vulnerable to collision risk, as small uncertainties in the initial position can quickly grow causing a high probability of collision. In this paper a framework for analysing the safety of a generic dispenser is proposed and applied to the study of a cylindrical dispenser. Through numerical simulations and linear covariance propagation, the evolution of the spacecraft state is retrieved and used for computing a set of performance metrics, such as the total probability of collision and the number of conjunction events. This method is then applied to a parametric analysis of the dispenser, examining how the performance metrics vary with parameters such as the velocity of release or the time between releases. The results thus obtained will be relevant to the safe design of spacecraft dispensers.

1 INTRODUCTION

Advances in rocketry and satellite manufacturing are changing the nature of the space industry and allowing new approaches to access space. A rapidly emerging example is the development and deployment of mega-constellations, consisting of 100s and 1000s of satellites operating as one network. The recent deployment of such systems is made possible by two key breakthroughs: the reduction in satellite mass and the lowering of the cost of accessing space. This, combined with the cost-per-kg falling from \$75,000/kg for space shuttle launches to LEO to just \$2,720/kg using a Falcon 9 [1], clearly shows how the barrier for launching multiple satellites together has lowered dramatically. This is demonstrated by the numerous Multiple Satellite Launches (MSLs) that currently are taking place around the world, ranging from the SpaceX Starlink and OneWeb satellites currently launched on a regular basis [2] to the record-breaking cases of 104 satellites deployed in 2017 by PSLV-C34 [3] and the 143 satellites released in orbit by the Space X Transporter-1 rideshare launch in 2021 [4]. Launching this many satellites comes with many risks, including the possibility of collision of the satellites after release. The release of multiple satellites is generally done by using a common dispenser through the release of gripping mechanisms or the use of springs. Immediately after the release, the satellites can remain in close proximity for many orbits. The risk of collisions in such early phases of MSLs arises from many factors. The uncertainty on the initial state of a satellite propagates

around the nominal trajectory. If the measurements are limited, the uncertainty grows. Following the release, even small uncertainties in the initial velocity and position can rapidly become large, corresponding to an increase in the probability of collision among spacecraft. If two satellites with high uncertainty share similar nominal trajectories, this generates many conjunction events where the probability of attempting to share the same position at the same time is high. The problem becomes even more challenging when the time window for releasing all the satellites is reduced to the minimum (e.g., just above 10 minutes for deploying 104 satellites, in the case of the PSLV-C34 launch in 2017 [3]) and the released spacecraft do not have any active orbit control onboard, as the case of many CubeSats that are generally launched as a secondary payload in these MSLs. In addition, in these phases, accurate tracking and orbit determination cannot be performed, since the satellites are closely packed together. The TLEs in these phases are unreliable as, in most cases, they do not allow for sufficient accuracy to distinguish one satellite from another. Whenever this is the case, it is critical that the release system can deploy spacecraft into safe trajectories which generate few or no conjunction events.

The aim of this paper is to develop a framework for assessing the safety of a given dispenser in the case of subsequent rapid releases of multiple spacecraft and to apply it to the parametric study of a cylindrical dispenser. The cylindrical case is analysed for similarity to existing dispensers like the SL-OMV [5] and the SHERPA models [6].

A similar problem is analysed in [7], where the collision risk for a cylindrical dispenser is given in terms of the average minimum distance across all released satellites and computed using a Monte-Carlo simulation. The framework is later extended in [8], where a numerical computation of the collision probability is introduced according to the work of [9]. In both these works, the parameter that is varied is the elevation of the velocity vector with respect to the circular plane of the dispenser. To avoid the use of Monte-Carlo simulations, [10] use a linear covariance propagation approach for computing the collision probability. An analytical method for computing the collision probability is given in [11] and it is described as more efficient compared to numerical methods in [12].

The collision risk for the released spacecraft from a common cylindrical dispenser flying in a nominal sun-synchronous orbit is analyzed here using a numerical simulation. Each simulation run is associated with a given set of parameters, which include the number of released satellites, the release velocity, the uncertainty on the velocity, the time between releases, the spin rate around the symmetry axis, and the initial attitude of the dispenser. The released satellites are then propagated numerically for their nominal orbits, while their covariance is computed using linear propagation as in [10]. The method in [11] is then used for computing the collision probability. The collision probability is then used as the basis of a series of risk metrics useful to judge the safety of the deployment for the given set of parameters. Multiple sets of parameters are analysed in multiple runs and compared to find drivers for the collision risk that will be useful for safe dispenser design.

The paper is structured in five sections. Section two contains a description of the scenario under investigation, including the type of analysed dispenser, its main parameters, the definition of the relevant reference frames, and all the relevant hypotheses for the underlying model of the simulation. Section three describes the main tools used for building the simulation, including a description of the linear covariance propagation method, the expression of the probability of collision, the definition of the performance metrics, and the structure of the underlying algorithm. In section four all the results from the parametric analyses are discussed, with a focus on the physical causes behind their behaviour with respect to the varying parameter. In section five all the relevant results are summarised and some observations on potential future developments are given.

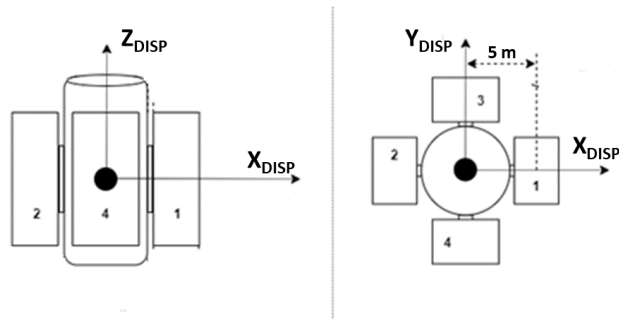


Figure 1: Scheme of the cylindrical dispenser

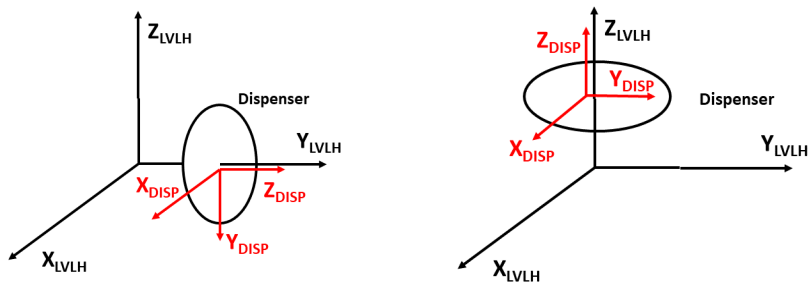


Figure 2: Attitude configurations: the axis of the dispenser is aligned with the trajectory on the left and it is perpendicular to the orbital plane on the right

2 SCENARIO DEFINITION

The aim of this section is to describe the scenario under investigation in this paper. We limit our focus to the SL-OMV and SHERPA-like dispensers. Such devices are constituted by a central cylinder that hosts payload adapters for the spacecraft to be deployed. In the following subsections, a description of the physical parameters of the test case dispenser is presented in Section 2.1, alongside the definition of all the reference frames, the hypotheses, and physical quantities necessary for describing the dynamics in Section 2.2.

2.1 Dispenser Parameters

The cases under investigation in this paper refer to the deployment of satellites in a sun-synchronous orbit. The reference orbit has an inclination of 98° , a relatively small eccentricity of 0.01, and an altitude of 700 km.

In order to simulate a representative case similar to the SL-OMV and the SHERPA models, a cylindrical dispenser is considered, with the spacecraft equally spaced all around the main body following a radial symmetry. A schematic representation of the dispenser is available in Fig. 1. The spacecraft are positioned at a radius of 5 m compared to the cylinder axis, to account for allocation of large spacecraft. The release velocity is always radial. Two different initial attitudes of the dispenser are analyzed in this paper. The first configuration considers the axis of symmetry of the cylinder aligned as the tangent to the trajectory, and the second configuration has the axis of symmetry of the cylinder perpendicular to the plane of the reference orbit, as shown in Fig. 2. All the relevant parameters are summarised in Table 1. Unless otherwise specified, all the simulations use the reference values.

Table 1: Dispenser Parameters

symbol	description	reference value
-	initial attitude	cylinder axis tangent to dispenser trajectory
n_{SC}	number of released spacecraft	4
dt	time between releases	10 s
v	release velocity	1 m/s
σ_v	standard deviation of release velocity	0.1 m/s
ω	spin rate around cylinder axis	0 rad/s

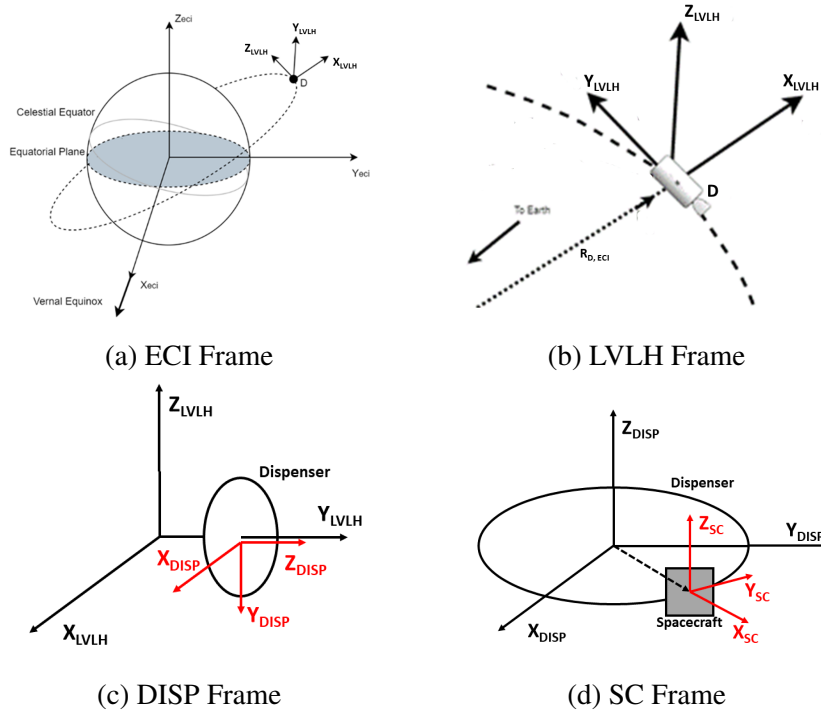


Figure 3: Reference frames

2.2 Simulation Hypotheses

All the orbits are propagated in an ECI (Earth-Centered Inertial) frame. The DISP (dispenser) reference frame is defined as the body frame centred at the dispenser's centre of mass and with the Z-axis aligned as the cylinder symmetry axis. All the initial positions of the spacecraft are defined in the DISP frame. The initial attitude of the dispenser is defined by the DCM (direction cosine matrix) of the DISP frame with respect to the LVLH (Local Vertical Local Horizontal) frame. The LVLH frame is centred at the centre of mass of the dispenser and defined with the X-axis in the direction of the dispenser position vector in ECI and the Z-axis in the direction of the angular momentum vector of the reference orbit. Since we consider near-circular orbits, the Y-axis is aligned very close to the tangential velocity of the dispenser's trajectory. The release velocity and its covariance matrix are defined in the SC (spacecraft) frame, centred at each spacecraft centre of mass with the X-axis in the direction of the spacecraft position vector in DISP and the Z-axis aligned with the Z-axis of DISP. All the relevant reference frames are shown in Fig. 3.

Given the initial conditions for the spacecraft position in the DISP frame $\mathbf{r}_{S,DISP}$, one can find the

position ECI using Eqs. 1:

$$\begin{aligned}\mathbf{r}_{S,LVLH} &= [R_{LVLH}^{DISP}]\mathbf{r}_{S,DISP} \\ \mathbf{r}_{S,ECI} &= \mathbf{r}_{D,ECI} + [R_{ECI}^{LVLH}]\mathbf{r}_{S,LVLH}\end{aligned}\quad (1)$$

where $[R_A^B]$ is the rotation matrix that goes from reference frame B to reference frame A and $\mathbf{r}_{D,ECI}$ is the position of the dispenser in ECI. Similarly, for the spacecraft initial velocity in the SC frame $\mathbf{v}_{S,SC}$ one can find its velocity in the ECI frame using Eqs. 2:

$$\begin{aligned}\mathbf{v}_{S,LVLH} &= [R_{LVLH}^{DISP}][R_{DISP}^{SC}]\mathbf{v}_{S,SC} + \boldsymbol{\omega} \times \mathbf{r}_{S,LVLH} \\ \mathbf{v}_{S,ECI} &= \mathbf{v}_{D,ECI} + [R_{ECI}^{LVLH}]\mathbf{v}_{S,LVLH} + \mathbf{n} \times \mathbf{r}_{S,ECI}\end{aligned}\quad (2)$$

where $\mathbf{v}_{D,ECI}$ is the velocity of the dispenser in ECI, $\boldsymbol{\omega}$ is the spin rate of the dispenser with respect to the LVLH frame, and \mathbf{n} is the angular velocity of the dispenser on its orbit as in Eq. 3.

$$\mathbf{n} = \frac{\mathbf{r}_{D,ECI} \times \mathbf{v}_{D,ECI}}{r_{D,ECI}^2}\quad (3)$$

The initial covariance matrices are given as in Eqs. 4:

$$[P_r]_{DISP} = \sigma_r^2 \begin{bmatrix} 1 & 0 & 0 \\ 0 & 1 & 0 \\ 0 & 0 & 1 \end{bmatrix}, \quad [P_v]_{SC} = \sigma_v^2 \begin{bmatrix} 1 & 0 & 0 \\ 0 & 1 & 0 \\ 0 & 0 & 1 \end{bmatrix}\quad (4)$$

where σ_r and σ_v are the standard deviations associated to the uncertainty of the initial position and velocity respectively. In this study $\sigma_r = 1$ cm, while the reference value of σ_v is available in Table 1. To rotate the covariance matrix it is useful to define the covariance matrix of the spacecraft state $\mathbf{x} = [\mathbf{r}^T, \mathbf{v}^T]^T$ in the DISP frame as in Eq. 5:

$$[P]_{DISP} = \begin{bmatrix} [P_r]_{DISP} & 0 \\ 0 & [P_v]_{DISP} \end{bmatrix}\quad (5)$$

where $[P_v]_{DISP}$ can be obtained from Eq. 6:

$$[P_v]_{DISP} = [R_{DISP}^{SC}][P_v]_{SC}[R_{DISP}^{SC}]^T\quad (6)$$

It is then possible to define two matrices $[R_1]$, $[R_2]$ as in Eqs. 7:

$$[R_1] = \begin{bmatrix} [R_{LVLH}^{DISP}] & [0] \\ [R_{LVLH}^{DISP}][\Omega] & [R_{LVLH}^{DISP}] \end{bmatrix}, \quad [R_2] = \begin{bmatrix} [R_{ECI}^{LVLH}] & [0] \\ [R_{ECI}^{LVLH}][N] & [R_{ECI}^{LVLH}] \end{bmatrix}\quad (7)$$

with $[\Omega]$ and $[N]$ defined from $\boldsymbol{\omega}$ and \mathbf{n} respectively as in Eqs. 8.

$$[\Omega] = \begin{bmatrix} 0 & -\omega_3 & \omega_2 \\ \omega_3 & 0 & -\omega_1 \\ -\omega_2 & \omega_1 & 0 \end{bmatrix}, \quad [N] = \begin{bmatrix} 0 & -n_1 & n_2 \\ n_3 & 0 & -n_1 \\ -n_2 & n_1 & 0 \end{bmatrix}\quad (8)$$

The covariances matrices in LVLH and ECI are then according to Eqs. 9.

$$\begin{aligned}[P]_{LVLH} &= [R_1][P]_{DISP}[R_1]^T \\ [P]_{ECI} &= [R_2][P]_{LVLH}[R_2]^T\end{aligned}\quad (9)$$

The nominal orbits are propagated according to a Keplerian model for 15 orbits (one day). The results in terms of uncertainties and probability of collision obtained with the Keplerian model are compared to a high-precision propagator accounting for Earth's oblateness and atmospheric drag perturbations to validate the accuracy. After each release, the spacecraft exchange momentum with the dispenser, changing its orbit slightly. Supposing one knows the release velocity of the spacecraft, the velocity of the dispenser after release can be computed according to the conservation of momentum as in Eq. 10:

$$\mathbf{v}_D^{(+)} = \frac{(m_D + m_S)\mathbf{v}_D^{(-)} - m_S\mathbf{v}_S^{(+)}}{m_D} \quad (10)$$

where m_D and m_S are the mass of the dispenser and of the spacecraft, respectively. For the specific case under analysis, we set to $m_D = 1000 \text{ kg}$ and $m_S = 10 \text{ kg}$ respectively. In Eq. 10, the terms $\mathbf{v}_D^{(-)}$ and $\mathbf{v}_D^{(+)}$ are the velocities of the dispenser before and after the release of the spacecraft, which on the other hand is released with a velocity $\mathbf{v}_S^{(+)}$.

3 METHODOLOGY

This section outlines the methodology of analysis adopted for propagating the uncertainty (Section 3.1), for calculating the probability of collision (Section 3.2), and for defining the performance metrics (Section 3.3) that will be then used in the simulation algorithm for assessing the impact of the different deployment strategies and initial conditions on the number of potential collisions and their probabilities.

3.1 Covariance Propagation

This investigation uses a Linear Covariance propagation strategy [12]. Specifically, under the assumption that the equations of motion can be linearized, the state of the system at any given time can be obtained from its initial state:

$$\mathbf{x}(t) = [\Phi(t, t_0)]\mathbf{x}(t_0) \quad (11)$$

where $\mathbf{x}(t) = [\mathbf{r}^T(t)\mathbf{v}^T(t)]^T$ and $\mathbf{x}(t_0) = [\mathbf{r}^T(t_0)\mathbf{v}^T(t_0)]^T$ represent the state of the released spacecraft composed by its position and velocity at time t and t_0 , respectively, and $[\Phi(t, t_0)]$ is the state transition matrix (STM) that relates the state at time t with the state at time t_0 .

Similarly, the covariance matrix at any given time can be calculated from the initial covariance using the STM as follows [12]:

$$[P(t)] = [\Phi(t, t_0)][P(t_0)][\Phi(t, t_0)]^T \quad (12)$$

Under the assumption that the reference orbit is near-circular and that the distances of the released spacecraft are always bounded by values much smaller than the reference orbit's radius, the STM can be calculated as:

$$[\Phi(t - t_0)] = \exp[[A](t - t_0)] . \quad (13)$$

where the matrix $[A]$ is given by the Chloessy-Wiltshire equations described in [13].

3.2 Collision Probability

The computation of the collision probability is performed through the analytical expression introduced by Chan and described in [12]. For a given couple of satellites at close approach, the probability of collision reads as:

$$P_C = \exp\left[-\frac{1}{2}\left(\frac{x^2}{\sigma_x^2} + \frac{y^2 + z^2}{\sigma_{yz}^2}\right)\right] \cdot \left[1 - \exp\left(-\frac{R_A^2}{2\sigma_x\sigma_{yz}}\right)\right] \quad (14)$$

where x, y, z are the coordinates of the secondary object in the LVLH frame defined by the primary object, σ_x and $\sigma_{yz} = \sqrt{\sigma_y^2 + \sigma_z^2}$ are the standard deviations of the covariance matrix obtained by the sum of the covariance matrices associated to the primary and secondary object, and R_A is a limiting distance for physical interference. In the specific case of this paper, we consider $R_A = 5 \text{ m}$. This formula holds for spacecraft pairs that are close to each other and for circular orbits in the Gaussian approximation for the covariance matrices. These hypotheses hold in this case as spacecraft released in rapid succession from a common dispenser stay close (less than 50 km) to each other for a long amount of time and the nominal orbit for the dispenser is almost circular.

3.3 Performance Metrics

The conjunction assessment is generally performed through the analysis of several quantities that represent how close and accurate are the predictions of collisions. The distance between pairs of satellites at each time step can be considered as the first and intuitive quantity to define a close encounter. For a given couple of satellites (i and j) this quantity is defined as:

$$\Delta r_{i,j}(t) = \|\mathbf{r}_i(t) - \mathbf{r}_j(t)\| \quad (15)$$

for each time instant t . Such a quantity can be used to define the number of conjunction events given a distance threshold D . In particular, whenever $\Delta r_{i,j} < D$ over a time interval, a conjunction event occurs within that interval. This metric, albeit intuitive, is not very useful in the scenario of a cluster of spacecraft released from a common dispenser. This is due to the fact that the satellites remain very close for a long amount of time, and therefore we might have situations where either the threshold is set too high, locating a single long conjunction event, or it is set too low, neglecting events that may have still a relevant probability of collision.

Another useful performance parameter is the minimum distance between each pair of satellites at any given time, defined as follows:

$$\Delta r_{min}(t) = \min_{i,j}[\Delta r_{i,j}(t)] \quad (16)$$

Such a parameter allows us to locate at what times the most critical events may occur, i.e. closer approach among all the possible couples of satellites.

A better way to detect and quantify high-risk events is to compute the probability of collision $P_C^{(i,j)}(t)$ for any pair of spacecraft (i, j) at any time t by using Eq.14. This definition allows us to redefine the conjunction events as those time intervals in which $P_C^{(i,j)}(t) > P_0$, being P_0 a threshold on the maximum probability of collision that we can consider acceptable. The advantage of this new definition is that one is certain to locate events that are not compliant with the acceptable probability of collision. For each pair of satellites (i, j), the total score of conjunction events given a simulation interval can be defined as $N_{conj}^{(i,j)}$. Therefore, the total number of conjunction events is the sum of the number of conjunction events over all satellite pairs for the entire interval of the simulation. This reads as:

$$N_{conj} = \sum_{i>j} N_{conj}^{(i,j)}. \quad (17)$$

The total probability of collision among all spacecraft pairs excluding the dispenser itself at each moment is defined as follows:

$$P_{C,tot}(t) = 1 - \prod_{i>j} (1 - P_C^{(i,j)}(t)) \quad (18)$$

Such a quantity is extremely useful to detect the most critical time intervals risk-wise for the whole system.

Finally, for each of the conjunction events it is possible to associate a maximum probability of collision as $P_{C,max}^{(k)} = \max_t [P_C^{(i,j)}(t)]$, with k being the identifier of the event and t taken within the time interval of the k -th event. In this way, it is possible to define the probability of at least one collision as follows:

$$P_{C,tot} = 1 - \prod_k (1 - P_{C,max}^{(k)}) \quad (19)$$

which, along with N_{conj} , can be used as an aggregate metric for assessing the risk of conjunctions in the whole system.

3.4 Simulation and Performance Assessment Algorithm

Algorithm 1 shows the procedure used for calculating the collision risk performance index for the selected test case scenarios. The obtained results will be described in Section 4, for different configurations and initial conditions, as thereby illustrated.

Algorithm 1 Simulation algorithm

Inputs: DispenserParameters, n_{SC} , $t_{R,k}$, t_f

Outputs: N_{conj} , $P_{C,tot}$

$k = 1$

while $n_{SC} > 0$ **do**

$\{\mathbf{x}_{k,0}, [P]_{k,0}\} = GetInitialConditions(DispenserParameters)$

$\mathbf{x}_k(t) = PropagateNominalState(\mathbf{x}_{k,0}, t_{R,k} : t_f)$

$[P]_k(t) = PropagateLinearCovariance([P]_{k,0}, t_{R,k} : t_f)$

$\mathbf{v}_{D,next} = VelocityAfterRelease(v_{D,prev})$

$\mathbf{x}_{D,next} = [\mathbf{r}_{D,next}^T, \mathbf{v}_{D,next}^T]^T$

$\{\mathbf{r}_{D,next}, \mathbf{v}_{D,next}\} = PropagateNominalState(\mathbf{x}_{D,next}, t_{R,k} : t_{R,k+1})$

$n_{SC} = n_{SC} - 1$

$k = k + 1$

end while

$[N_{conj}, P_{C,tot}] = GetPerformanceMetrics(\mathbf{x}_k(t), [P]_k(t))$

In the code, the following top-level tasks are defined:

- *GetInitialConditions(DP)* transforms the dispenser parameters DP into the initial conditions on the state and covariances for all the released spacecraft.
- *PropagateNominalState*($\mathbf{x}_0, t_i : t_f$) propagates the initial state x_0 from t_i to t_f according to a Keplerian model.
- *PropagateLinearCovariance*($[P]_0, t_i : t_f$) propagates the initial covariance $[P]_0$ from t_i to t_f according to the linear model.
- *VelocityAfterRelease*(v_{prev}) updates the velocity of the dispenser after release due to the conservation of momentum.
- *GetPerformanceMetrics*($\mathbf{x}(t), [P](t)$) computes the performance metrics for the given nominal state vector and the given vector of covariance matrices.

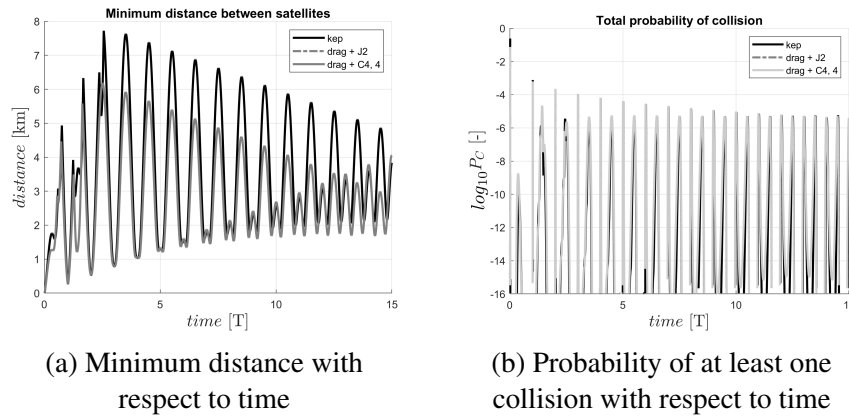


Figure 4: Results for the base case in the Keplerian case and with Earth oblateness and drag effects

4 RESULTS

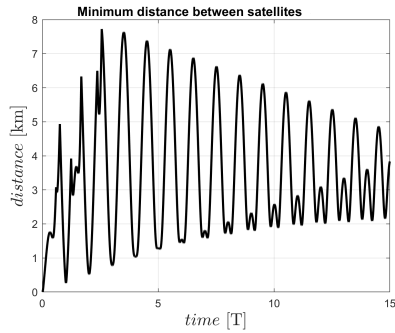
This section contains the results of the parametric analyses. The results are discussed with respect of the physical causes driving the behaviour of the performance metrics with respect to the varying parameters.

4.1 Baseline case

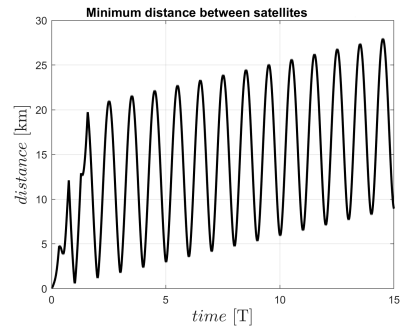
The baseline case refers to the parameters of Table 1. The results are shown in Fig. 4, where the behaviours of the minimum distance and the total probability of collision are represented in Fig. 4a and 4b, respectively. Over the 1-day time window, the minimum distance among all spacecraft is always under 8 km, which means that there is always at least one pair of satellites that are nearer than 8 km at some point in their nominal orbits. The probability of collision has a large spike at the beginning, and it peaks after every full orbit, but after three orbits it decreases below 0.01%. The initial peak on the total probability of collision reaches 10% and it is due to the very short release time interval among the spacecraft. The same figures show a comparison between the Keplerian model, used for propagating the uncertainties, and more accurate models that account for Earth's oblateness and atmospheric drag. Despite substantial differences in the observed minimum distance, the behavior of the probability of collision is qualitatively the same and it does not yield any new information compared to the Keplerian case.

4.2 Initial attitude

Figures 5 and 6 show the minimum distance and the total probability of collision in the cases where the dispenser's axis of symmetry is aligned with the trajectory, Fig. 5a and Fig. 6a, and perpendicular to the orbital plane, Fig. 5b and Fig. 6b, respectively. The second case yields a much lower total probability of collision while having a much higher minimum distance between satellites. This suggests that the critical spacecraft couples are those involving satellites with an out-of-plane component of the velocity. This follows from the basic physics of the system, as the in-plane components of the velocity introduce a drift which progressively increases the distance between the satellite couples. On the other hand, the spacecraft with out-of-plane components of the velocity oscillate around the nominal orbit, as the periods of the orbits of the released spacecraft remain approximately the same. The best strategy for minimising the collision risk is therefore to release the spacecraft in the plane of the nominal orbit.

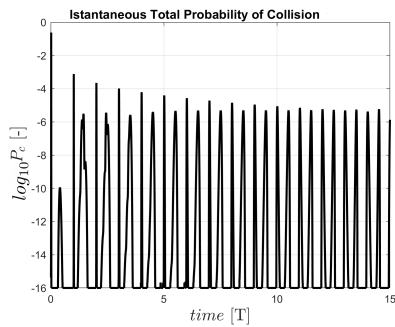


(a) Minimum distance, axis aligned with trajectory

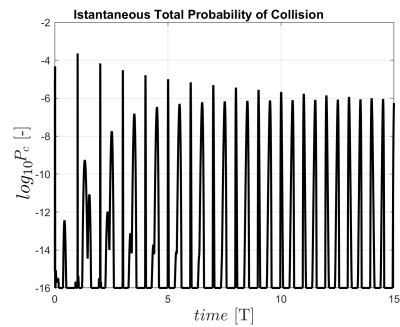


(b) Minimum distance, axis perpendicular to orbital plane

Figure 5: Minimum distances for the two attitude configurations

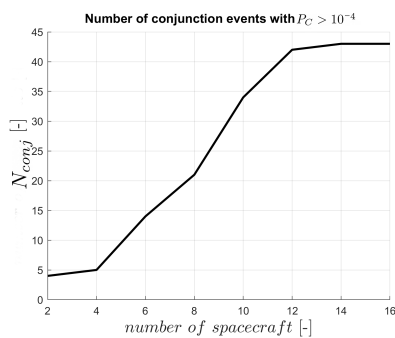


(a) Probability of at least one collision, axis aligned with trajectory

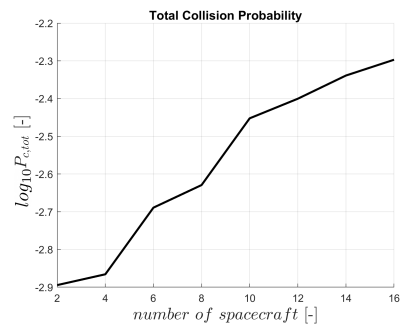


(b) Probability of at least one collision, axis perpendicular to orbital plane

Figure 6: Total probabilities of collision for the two attitude cases



(a) Number of conjunction events



(b) Probability of at least one collision

Figure 7: Results for varying number of released spacecraft

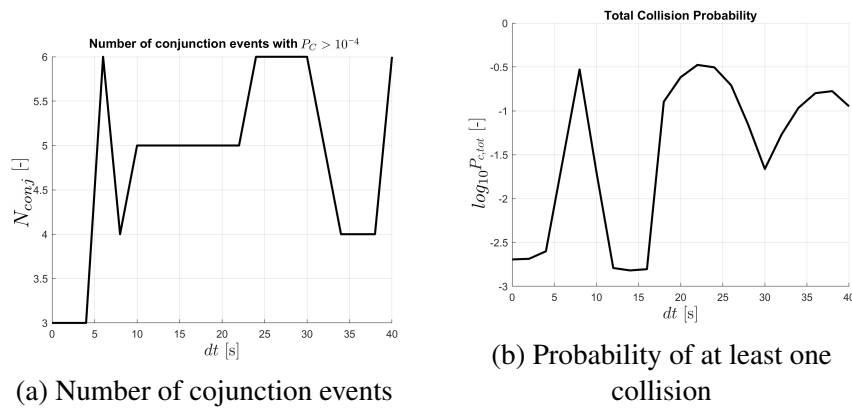


Figure 8: Results for varying time between releases

4.3 Number of spacecraft

The performance indices of the system change as expected if the number of released spacecraft increases. This is demonstrated by the analysis of Fig. 7. In this case, the number of released spacecraft, disposed in radial symmetry on the dispenser, is varied from 2 to 16. As expected, the logarithm of the total collision probability and the number of conjunction events increase almost linearly with the number of spacecraft. This is intuitive, as the spacecraft are more packed together initially and produce more chances for close encounters.

4.4 Time between releases

Figure 8 shows the number of conjunction events with $P_C > 10^{-4}$ as a function of the time interval between the release among spacecraft, Fig. 8a, and the corresponding total probability of collisions for the whole simulation, Fig. 8b. In this case, the time between releases is varied between 0 and 40 s, with 0 s representing the case of simultaneous release. No explicit correlation of the performance metrics with the time between releases could be found. Releasing the spacecraft rapidly one after the other yields the advantage of cutting off the initial spike in the collision probability, at the expense of having the spacecraft very close for the whole time window, as shown in Fig. 9. Having a high time between releases, on the contrary, reduces the conjunction time intervals, with the drawback of an increasingly lower minimum distance front due to the higher oscillations, as shown in Fig. 10. Due to the absence of drift, this effect is likely attributable to the fact that satellites with out-of-plane components of the velocity become the main driver of collision probability and their dynamics is largely independent of the time of release.

4.5 Velocity of release

Figure 11 shows the results of the parametric analysis performed by varying the release velocity. In this case, the magnitude of the velocity of release is varied between 0.2 and 2 m/s. As expected, the total number of conjunction events greatly decreases with the higher release velocity. This is intuitive because the higher the release velocity, the more distanced the satellites become, yielding fewer chances of close encounters. The total collision probability follows a less obvious pattern, but this could be due to the assumptions and approximations made for its computation, as the variation is very small. In this case, the number of conjunction events are likely a more relevant metric.

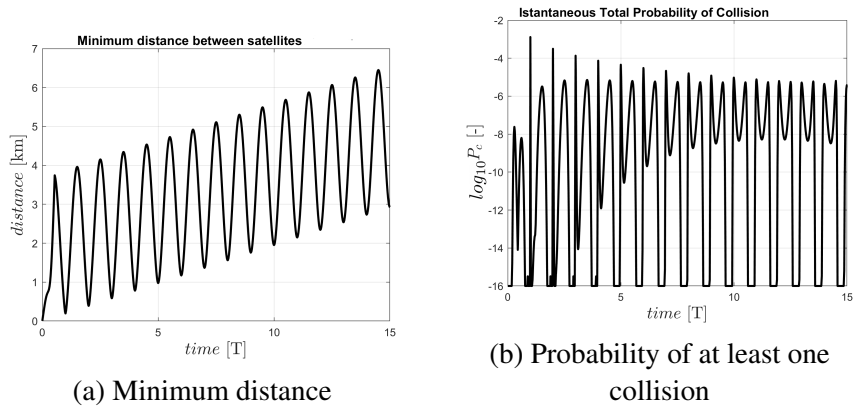


Figure 9: Results for $dt = 0$ s

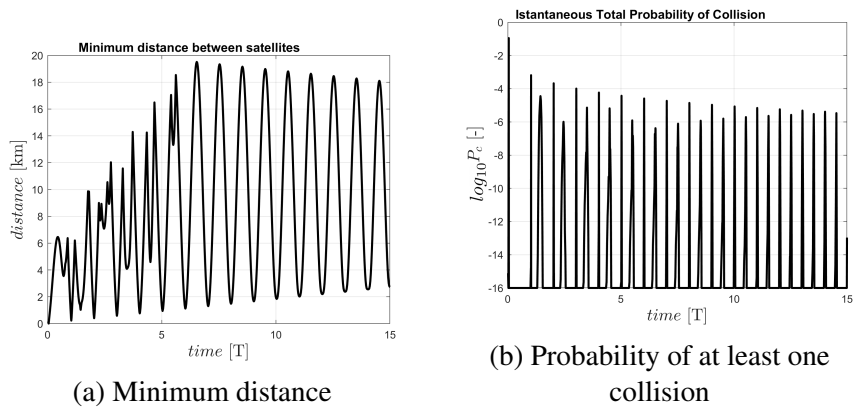


Figure 10: Results for $dt = 40$ s

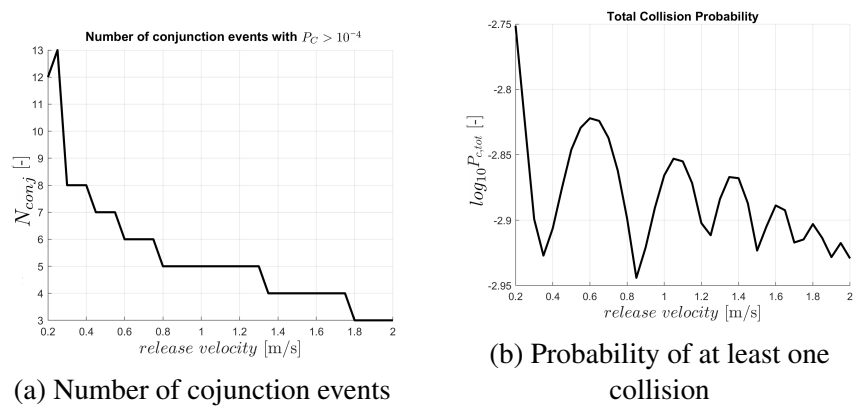


Figure 11: Results for varying velocity of release

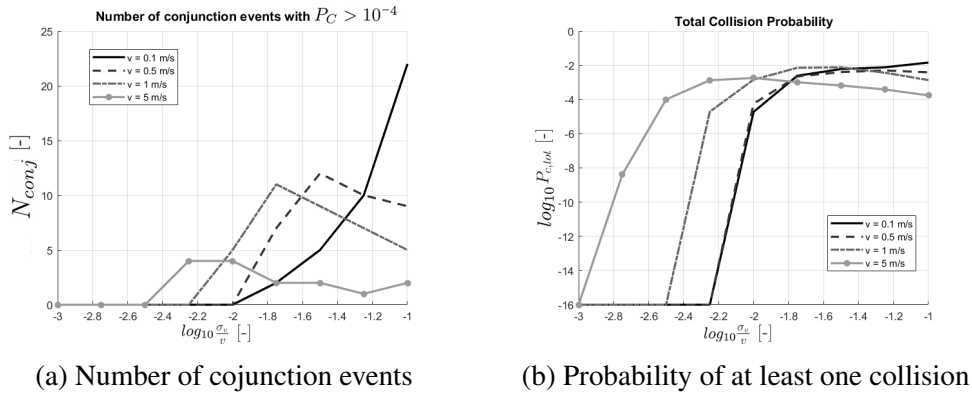


Figure 12: Results for varying uncertainty on the velocity of release

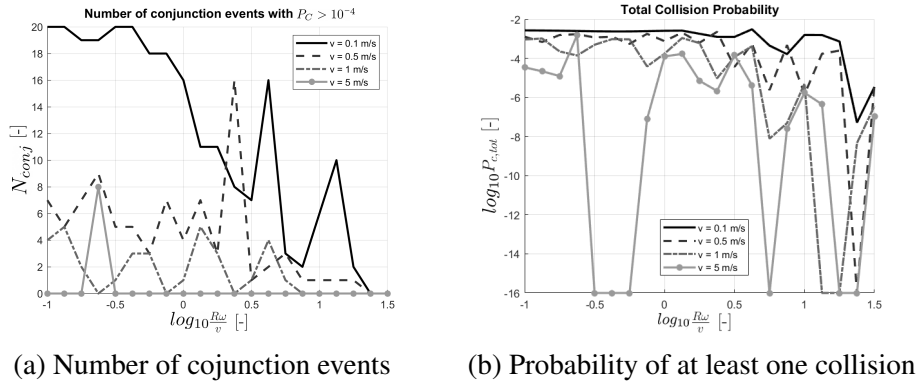


Figure 13: Results for varying spin rate

In a second study, the standard deviation associated to the release velocity was varied along with four cases of velocity. In particular, $\frac{\sigma_v}{v}$ was varied from 10^{-3} to 10^{-1} . The results, shown in Fig. 12, depend more on the value of σ_v than the value of $\frac{\sigma_v}{v}$. Whenever $\sigma_v < 0.01$ m/s, the total probability of collision drops significantly. The number of conjunction events follows a similar behaviour. This should not come as a surprise, as the covariance, and therefore the probability, exhibits no explicit dependency on the velocity. A curious observation is that for high standard deviation, the total probability of collision decreases slightly, against intuition. This is likely due to the dilution of probability, a phenomenon where a very high covariance can paradoxically yield a decrease in the probability of collision. This effect is explained in detail in [14].

4.6 Spin rate

The effect of an added spin rate around the cylinder axis is shown in Fig.13. First, the performance was analysed with respect to the non-dimensional parameter $\frac{R\omega}{v}$, where R is the radius of the cylindrical dispenser, v is the magnitude of the release velocity, and ω is the spin rate. The performance was analysed for four fixed values of v . It is possible to observe that, although for small values of $\frac{R\omega}{v}$ the effect of the spin rate is negligible compared to the effect of the release velocity, consistent improvements of the number of conjunction events and total collision probability are possible for $\frac{R\omega}{v} > 1$. The oscillatory behaviour notable at large velocities is likely due to a synchronisation between the spin period and the time of release. In particular, for specific values of the spin rate, spacecraft may be released in favourable geometries. This effect can be better observed when studying the perfor-

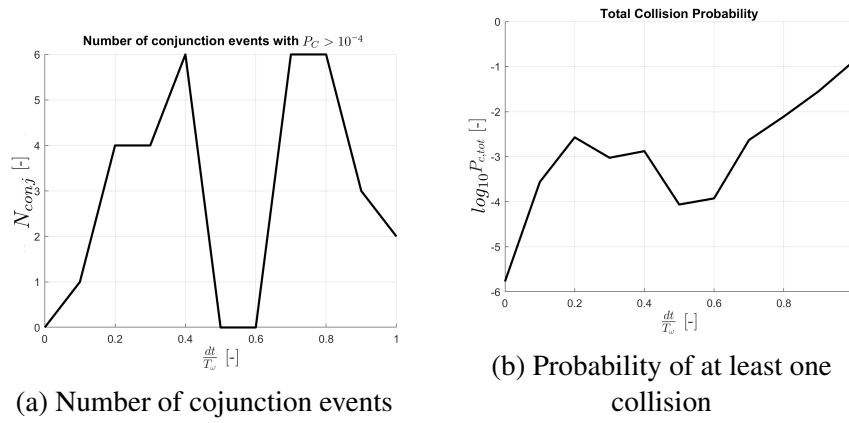


Figure 14: Results for time between releases compared to the spin period, $\omega = 0.05\pi$ rad/s

mance behaviour with respect to $\frac{dt}{T_\omega}$, where dt is the time between releases and T_ω is the period of the spinning cylinder. The analysis was performed for a fixed value $\omega = 0.05\pi$ rad/s. The results are shown in Fig. 14. In this case the number of conjunction events is maximised around $dt = \frac{T_\omega}{4}$, where spacecraft are released in rapid succession in the same direction.

5 CONCLUSION

In this paper, the performance with respect to collision risk for a cylindrical dispenser carrying multiple spacecraft released in rapid succession was analysed. Supposing initial uncertainties on the position and velocity of the released spacecraft, the covariance was propagated linearly using the Clohessy-Wiltshire equations for relative orbital motion. The propagated nominal positions and covariances were then used to compute the probability of collision at each time step. The resulting probability of collision was then used for computing the total number of conjunction events and the total probability of collision for the whole system. When varying the initial attitude, the most favourable case was found to be the one with the axis of the dispenser perpendicular to the plane of the orbit. As expected, an increase in the number of released spacecraft yielded an increase in the number of conjunction events and total probability of collision. A reduced release time yielded a lower initial peak in the probability of collision. For a fixed number of spacecraft, the most influencing factor was the release velocity: higher release velocities cause the spacecraft to better distance themselves, avoiding conjunction events. On the contrary, no obvious advantage was found for decreasing the uncertainty on the release velocity while keeping its standard deviation over 0.01 m/s. The introduction of a spin rate is beneficial for a small time between releases due to the added component of the velocity, but it may potentially decrease performance when synchronisation between release velocity and spin period arise. The findings of this paper inform on the main drivers of collision risk for the safe design of multiple spacecraft dispensers. Although many parametric analyses were run, it is possible that there are yet more interactions between the dispenser parameters in terms of how they influence operation safety. Future research should focus on more detailed and fine-grained parametric analyses, possibly on a longer time window. Where this may become too computationally expensive, novel techniques could be explored for researching an optimal set of dispenser parameters in terms of safety. Due to the multiple assumptions made for producing this testing framework, further research may be considered regarding how to improve these models and when these assumptions fail yielding to performance metrics not mirroring physical behaviour. Lastly, some validation based on real data will be required to assess the limitations of the model underlying simulation frameworks such as the one developed for this study.

REFERENCES

- [1] H. W. Jones, “The recent large reduction in space launch cost,” *48th International Conference on Environmental Systems*, 2018.
- [2] C. C. Helms, “A survey of launch services 2016-2020,” *AIAA Propulsion and Energy 2020 Forum*, DOI: 10.2514/6.2020-3532.
- [3] space.com. “India launches record-breaking 104 satellites on single rocket.” (2017), [Online]. Available: <https://www.space.com/35709-india-rocket-launches-record-104-satellites.html> (visited on 05/28/2023).
- [4] EOportal. “Transporter-1.” (2021), [Online]. Available: <https://www.eoportal.org/other-space-activities/transporter-1#record-rideshare-launch-challenges> (visited on 05/28/2023).
- [5] Moog. “Sl-omv space vehicle tug.” (2021), [Online]. Available: <https://www.moog.com/products/space-vehicles/sl-omv.html> (visited on 05/28/2023).
- [6] Spaceflight.com. “Sherpa program: New orbital transfer vehicles launch smallsats to custom orbital destinations.” (2022), [Online]. Available: <https://spaceflight.com/sherpa/> (visited on 05/28/2023).
- [7] F. Santoni, F. Piergentili, and R. Ravaglia, “Collision risk analysis for nanosatellite cluster launches,” *61st International Astronautical Congress*, 2010.
- [8] F. Santoni, F. Piergentili, and R. Ravaglia, “Nanosatellite cluster launch collision analysis,” *Journal of Aerospace Engineering*, vol. 26, pp. 618–627, 2013. DOI: 10.1061/(ASCE)AS.1943-5525.0000175.
- [9] S. Alfano, “A numerical implementation of spherical object collision probability,” *The Journal of the Astronautical Sciences*, vol. 53, pp. 103–109, 2005. DOI: 10.1007/BF03546397.
- [10] S. H. Hur-Diaz, M. C. Ruschmann, M. Heyne, and M. R. Phillips, “Computing collision probability using linear covariance and unscented transforms,” *AIAA Guidance, Navigation, and Control (GNC) Conference*, 2013. DOI: 10.2514/6.2013-5189.
- [11] K. Chan, “Short-term vs. long-term spacecraft encounters,” *AIAA/AAS Astrodynamics Specialist Conference and Exhibit*, 2004. DOI: 10.2514/6.2004-5460.
- [12] L. Chen, X. Bai, Y. Liang, and K. Li, *Orbital Data Applications for Space Objects*. Springer, 2017.
- [13] W. H. Clohessy and R. S. Wiltshire, “Terminal guidance system for satellite rendezvous,” *Journal of the Aerospace Sciences*, vol. 27, pp. 653–658, 1960. DOI: 10.2514/8.8704.
- [14] M. S. Balch, “A corrector for probability dilution in satellite conjunction analysis,” *18th AIAA Non-Deterministic Approaches Conference*, 2016.